We are IntechOpen, the world's leading publisher of Open Access books Built by scientists, for scientists

6,900
Open access books available

185,000
International authors and editors

200M
Downloads

Our authors are among the

154
Countries delivered to

TOP 1%
most cited scientists

12.2%
Contributors from top 500 universities

WEB OF SCIENCE™

Selection of our books indexed in the Book Citation Index in Web of Science™ Core Collection (BKCI)

Interested in publishing with us?
Contact book.department@intechopen.com

Numbers displayed above are based on latest data collected.
For more information visit www.intechopen.com

Chapter 11

Raman Spectroscopy with X-Rays

Piter Sybren Miedema

Additional information is available at the end of the chapter

http://dx.doi.org/10.5772/65427

Abstract

The Raman effect in the X-ray wavelength regime as applied to spectroscopy is described in this chapter: The concepts of these X-ray Raman spectroscopies, (nonresonant) X-ray Raman spectroscopy, and resonant X-ray Raman spectroscopy, better known under the name resonant inelastic X-ray scattering, have been shortly described, and this chapter further focuses on (why) using these spectroscopic methods by showing some current applications of these techniques. As well, some possible future applications are mentioned.

Keywords: X-ray Raman spectroscopy, resonant inelastic X-ray scattering (RIXS), synchrotrons, X-ray free-electron lasers, X-ray absorption spectroscopy, X-ray emission spectroscopy

1. Introduction

Raman spectroscopy studies are commonly employed in the UV and visible light (UV-VIS) regime, making use of an easily available monochromatic UV-VIS (laser) incoming beam and measuring energy losses (or energy gains) related to vibrational and rotational states of the system of interest. As such, Raman spectroscopy is used in chemistry to provide fingerprints by which molecules can be identified. The principle of Raman spectroscopy is the Raman effect of a photon upon interaction with matter: when a photon is scattered from an atom or molecule (or crystal), a small fraction of the scattered photons are scattered by an excitation, with the scattered photons having an energy different from that of the incident photons. In most cases, the scattered energy is lower, which is called Stokes Raman scattering, and in the less common case, when the scattered energy is increased, it is called anti-Stokes Raman scattering. Thus, Raman relies on inelastic scattering (Raman scattering) of monochromatic light, usually from a laser in the visible, near-infrared, or ultraviolet range.

INTECH
open science | open minds

© 2017 The Author(s). Licensee InTech. This chapter is distributed under the terms of the Creative Commons Attribution License (http://creativecommons.org/licenses/by/3.0), which permits unrestricted use, distribution, and reproduction in any medium, provided the original work is properly cited. CC BY

However, based on the basics of the Raman effect mentioned above, there is no reason why the Raman effect should not be present in other wavelength regimes, and this chapter deals with the Raman analogues in the X-ray regime: X-ray Raman spectroscopy (XRS) and resonant X-ray Raman spectroscopy or the more commonly used term resonant inelastic X-ray scattering (RIXS). This chapter provides details concerning this X-ray regime Raman spectroscopy being not only a fingerprint for molecules but even an element-dependent electronic structure fingerprint. In general, X-ray spectroscopies may supply electronic structure information on element-specific oxidation and spin states.

As well as for the UV-VIS regime, XRS and RIXS can deal with vibrational or phonon energy losses and/or gains, which will only be shortly discussed in Section 3. Besides, since X-ray photons have much higher energy than UV-VIS photons, one may observe much bigger energy losses, which will be explained in detail in Section 3. Some applications of XRS will be covered in Section 4. In Section 5, RIXS will be explained and Section 6 shows some applications of RIXS spectroscopy. But at first we take a step back in Section 2, where some basics on X-ray spectroscopies in general are covered.

2. Some basics about X-ray spectroscopies – absorption spectroscopy

While moving in the wavelength regime from UV-VIS to X-rays, one must realize that X-ray photons have substantially more energy than UV-VIS photons. Whereas UV-VIS photons above certain energy can excite valence electrons into the conduction band, the energy of X-ray photons can be applied to excite core electrons into the conduction band. In general, the unit electronvolt (eV) is used in X-ray spectroscopies, which corresponds to 1 eV = 1.60210 × 10^{-19} J = 8065.73 cm^{-1}. As for other absorption spectroscopies, X-ray absorption spectroscopy (XAS) is a matter of measuring the difference between the intensity of the incoming beam and transmitted beam following the Lambert–Beer's law:

$$I_t = I_0 e^{-\mu y} \tag{1}$$

where t is the sample thickness and μ is the absorption coefficient. I_t is the transmitted intensity and I_0 is the incoming intensity. For XAS, the absorption coefficient μ gives the probability that X-rays will be absorbed. At most X-ray energies, the absorption coefficient is a smooth function of energy, with a value that depends on the sample density ϱ, the atomic number Z, atomic mass A, and the X-ray energy E roughly as:

$$\mu \approx \frac{\rho Z^4}{AE^3} \tag{2}$$

The strong dependence of μ on both atomic number Z and energy E is a fundamental property of X-rays. With X-ray spectroscopies, one can gain information about selected elements by

choosing the right X-ray energy range; due to the high energy of X-ray photons, these photons may lead to the excitation of core electrons to unoccupied levels. The energy of these core electron levels is determined by the type of element. That is, in a nutshell why X-ray absorption-related spectroscopies are element-specific. As an example the X-ray transmission of cobalt and iron is shown in **Figure 1** for sample thicknesses of 0.2 μ. The energy level of the iron 1s core level is at about 7112 eV (black dotted line in **Figure 1**), and the energy level of the next neighbor in the periodic table cobalt 1s lies at about 7709 eV (red solid line in **Figure 1**) as can be seen from the decrease in the transmission of X-rays around this energy. A difference of 600 eV is substantial keeping in mind that 1 eV corresponds to 8065.73 cm^{-1}.

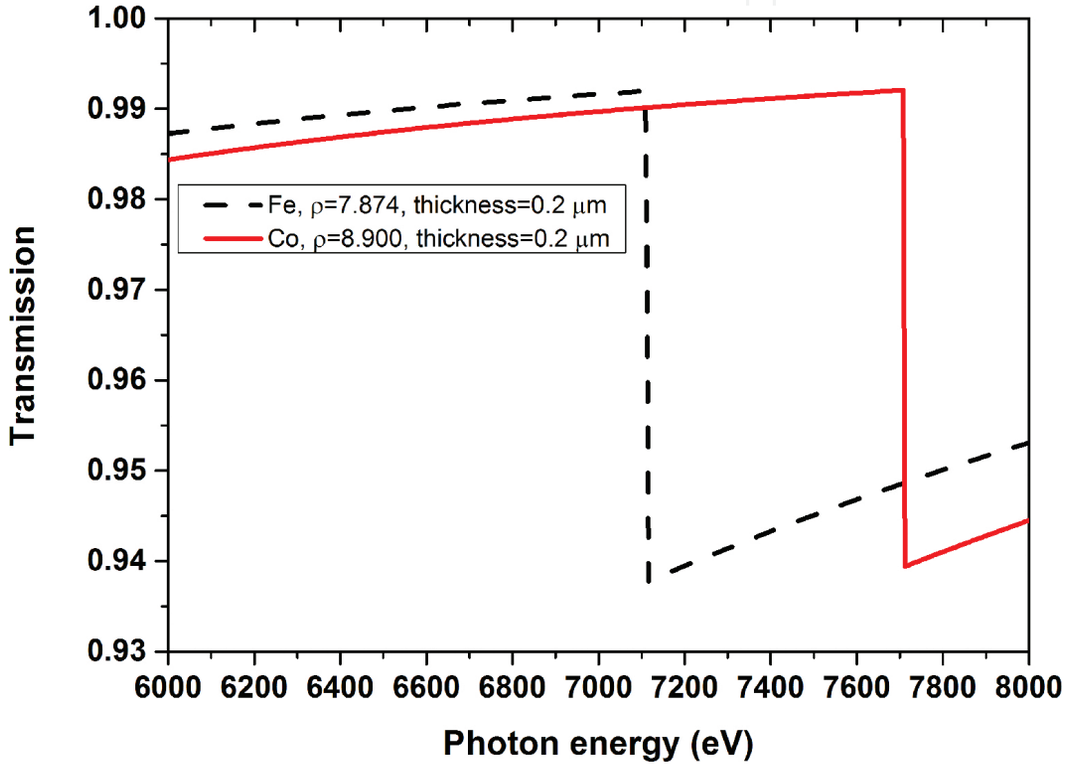

Figure 1. X-ray transmission for iron and cobalt with thicknesses of 0.2 μm as available from CXRO (henke.lbl.gov/optical_constants/filter2.html).

One prerequisite for XAS (and as well for many other X-ray spectroscopies) is a widely energy-tunable X-ray source, and in general, synchrotron radiation is required. Table-top tunable X-ray sources are coming up as well, but the required brilliance for photon-in photon-out spectroscopies such as XRS and RIXS is only available at synchrotrons and X-ray free-electron lasers (X-ray FELs). For an overview of available synchrotrons and FELs, see www.lightsources.org.

Because the core-level energies are so different for different types of atoms, it means that the absorption of an X-ray photon is element-specific. In addition, many X-ray spectroscopies are as well able to identify relative oxidation states (see for example Refs. [1, 2]) and spin states (see for example Refs. [1, 3, 4]). For the heavier elements, there will be more than one core

level. For example, for the previously mentioned iron, there is the 1s core level (K-edge), and 2s (L_1-edge), and 2p levels ($L_{2,3}$-edge), and the 3s (M_1-edge) and 3p levels ($M_{2,3}$-edge) may also be considered as core levels. The word "edge" comes historically from the fact that at certain X-ray energies, there is a steep change in absorption: these sharp rises in X-ray absorption (or deep decreases in X-ray transmission as seen in **Figure 1**) are due to reaching the binding energy of a certain core level. The edges are named after the excited core-level electron as indicated in between brackets above (K-edge, L-edge, etc.).

From the chemistry perspective, one would like to use the X-ray edge, which is sharpest with the best energy resolution or in other words with the best chemical resolution. These "best chemical resolution edges" appear for all elements between 40 and 1000 eV [5], in the so-called (VUV to) soft X-ray regime.

In general, X-ray energies above 2000 eV are considered to be part of the hard X-ray regime. The energy region between 1000 and 2000 eV is some intermediate tender X-ray regime, which is sometimes considered to be a separate part and sometimes part of either the soft X-ray regime or the hard X-ray regime. The terms hard X-ray and soft X-ray refer to their penetration depth in air. Soft X-ray photons below 1000 eV do not penetrate far through air (due to absorption by CO_2, O_2, and N_2), and that is why in the soft X-ray regime, measurements are normally performed under vacuum. Hard X-rays do penetrate through air, and in this regime, Röntgen originally discovered X-ray radiation. As hard X-rays do penetrate through air, experiments with hard X-rays normally are performed with safety lead shields around the experiment in order to absorb the hard X-rays and protect the surrounding, for example, the spectroscopists/scientists from exposure to X-rays.

Note that in hospitals, they actually make use of the penetration depth of hard X-rays for X-ray CT scans: since bones absorb stronger than other parts of the human body, but still a substantial part of the incident X-ray beam is completely transmitted through the body, this CT scan tells you something about bone breaking.

As mentioned previously, the best chemical resolution edges are in the soft X-ray regime and this X-ray regime has limits on the measurement conditions: in general high vacuum operation conditions (below 10^{-7} mbar), although there are developments into operation under milder vacuum conditions, for example, soft X-ray emission on liquids in the 10^{-3} mbar regime [6] and X-ray photoelectron and electron yield X-ray absorption spectroscopy on solids in the 1 mbar [7–9] to 1 bar regime [10].

In the next section, it will become clear how X-ray Raman spectroscopy circumvents the constraints of the soft X-ray regime, while still leading to spectra that resemble the soft X-ray edge with the best chemical resolution.

3. X-ray Raman spectroscopy

X-ray Raman Spectroscopy (XRS) or nonresonant inelastic X-ray scattering (NIXS) is a spectroscopy that makes use of the Raman concept as sketched in **Figure 2**; there is a mono-

chromatic incoming X-ray beam with energy E_0, and the scattered X-rays are measured as function of the emitted energy E_f. The incoming and scattered X-rays do not have to directly correspond to an X-ray edge; however, the Raman energy loss ΔE due to a scattering event may be related to some core-level excitation (or to phonon excitation like in typical Raman spectroscopies).

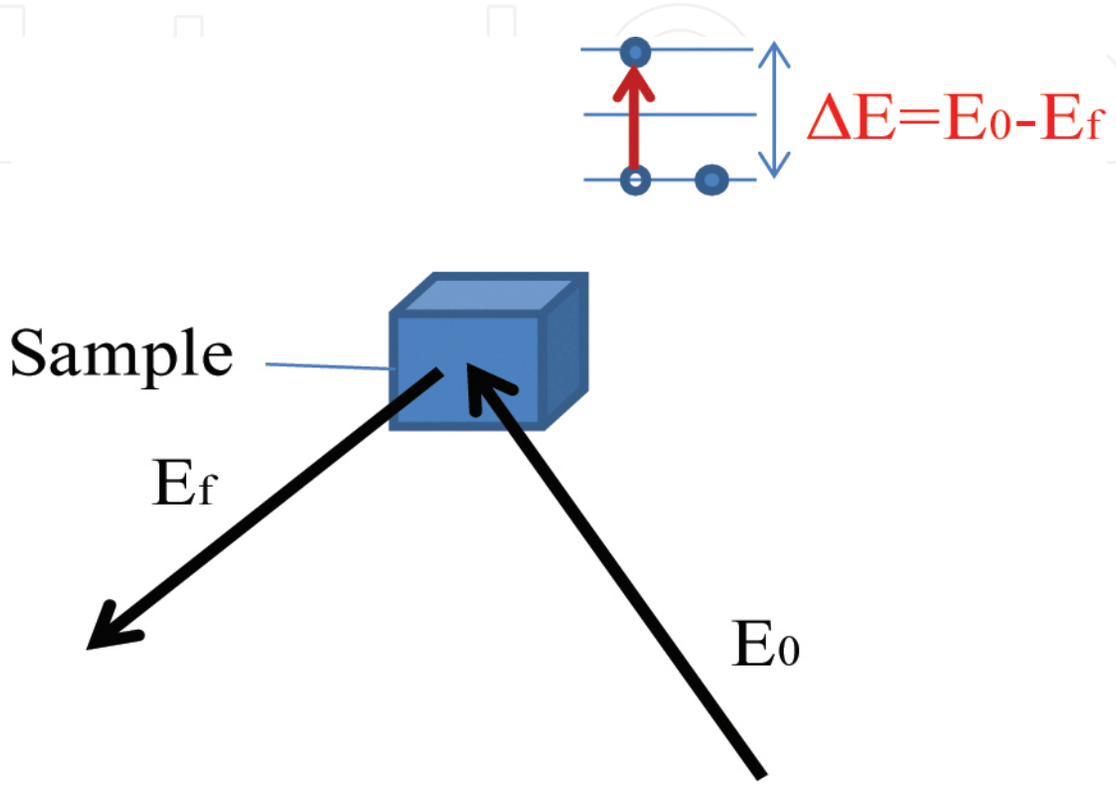

Figure 2. Schematic representation of the X-ray Raman process.

Note that in this scattering process, there are other events which are much more likely, elastic (Rayleigh) scattering and Compton scattering (see for example the relative intensities in **Figure 1** of Ref. [11]). Initially, the low cross section of XRS made this technique impractical, but intense new X-ray facilities, third-generation synchrotrons and X-ray free-electron lasers (FELs), and improvements in X-ray optics helped XRS to become an interesting spectroscopic tool.

XRS is a technique that retains the experimental advantages of hard X-ray measurements, for example, deeper probing depth implying more realistic samples, less beam damage due to lower scattering cross section, experiments in a gas or liquid environment or under higher pressures, while revealing the information equivalent to the soft X-ray XAS. In particular, for K-edges of the light-weight elements, which have really low VUV to soft X-ray energies as their edge, leading to a substantial low penetration depth, XRS can circumvent the problems related to soft X-rays. The difference between XRS and XAS is the transition operator. In XAS, the electronic transition can be approximated as a dipole transition, while for XRS also higher-order transitions (quadrupole) are allowed, depending on the q-vector, related to the angle

between incident and scattered X-rays. At low values for q, only dipole transitions are allowed, so far low-q XRS compares well with XAS. For high-q, higher-order transitions are present in XRS, which will be shortly discussed in the next section.

XRS, RIXS, and nonresonant X-ray emission spectroscopy (XES), where RIXS and XES will be discussed in more detail later on, are second-order optical processes where the excitation and de-excitation processes are coherently correlated by the Kramers-Heisenberg formula depicted here:

$$F(\Omega,\omega) = \sum_j \left| \sum_i \frac{\langle j|T_2|i\rangle\langle i|T_1|g\rangle}{E_g+\hbar\Omega-E_i+i\Gamma_i} \right|^2 \delta(E_g + \hbar\Omega - \mathrm{E}_j - \hbar\omega) \tag{3}$$

Where $\hbar\omega$ and $\hbar\Omega$ are the energies of the incident X-ray and emitted/scattered X-ray energy, respectively. j, i, and g present the final, intermediate, and ground states, respectively. T_1 and T_2 represent the radiative transitions by incident and emitted photons, and Γ_i represents the spectral broadening due to the core-hole lifetime in the intermediate state. δ is the energy conservation of the process with difference in the ground state energy plus the X-ray emitted energy with the final state energy plus the incident X-ray energy. As this formula shows there is a dependence on the core-hole lifetime, which can be made use of to study core-hole state dynamics in RIXS spectroscopy (discussed later in Section 6).

In electron spectroscopies, a spectroscopy equivalent to XRS exists, which is called electron energy-loss spectroscopy (EELS). Both XRS and EELS give information similar to XAS, but because the transitions in XRS and EELS occur in a different way, the transition operator is different. However, at low momentum transfer (low q-vector), the transition operator in EELS and XRS can be approximated as a dipole operator, and in that case, the spectral shape agrees with XAS.

XRS can be measured in two modes: (A) the direct analogue of common Raman spectroscopy: a monochromatic X-ray beam is used and the emitted X-ray beam is measured as function of energy loss (or emission energy). (B) The emitted X-ray energy is fixed and the incoming X-ray beam is varied, the so-called inverse energy scan technique. Currently, mode B is applied more often since it is easier to change the incoming monochromatic energy than the settings of the emission spectrometer for different emission energies; however, with dispersive X-ray emission spectrometers [12], mode A may become the standard mode, which would be beneficial for (femtosecond) time-resolved studies with X-ray FELs.

Besides the use of XRS as some correspondence spectroscopy to XAS, one can also measure low-loss features such as phonons (vibrations for molecules) and plasmons as with traditional Raman spectroscopy. In this meV energy-loss scale, the technique is actually often called as NIXS or IXS. The advantage of NIXS compared to traditional (UV-VIS regime) Raman spectroscopy is that the X-rays penetrate deeper in materials than UV-VIS photons, so the energy loss obtained related to phonons and plasmons with NIXS might give a more bulk-like picture of the phonon and plasmon behavior of the system of interest. As well a wider energy

and momentum space can be probed with synchrotron radiation. This NIXS will not be discussed further, one is referred to Refs. [13–16].

4. Some applications of X-ray Raman spectroscopy

4.1. *In situ* X-ray spectra of light elements

XAS of light elements, such as lithium (Li), boron (B) and carbon (C), occurs in the soft X-ray energy range at about 60, 180, and 280 eV, respectively. In general, XAS can be measured in transmission, electron, or ion yield or fluorescence yield mode. Due to the path lengths of soft X-rays, transmission X-ray absorption measurements in this soft X-ray energy range of 50–300 eV are very difficult. The electron yield mode of XAS is an alternative surface-sensitive measure for the standard transmission XAS mode. Concerning *in situ* XAS studies, it can as yet only be performed at the mbar to bar pressure range, for example, as shown in Refs. [7, 9]. Fluorescence yield XAS probes deeper into the sample, but this probe has very low yield for soft X-ray energies and may suffer from saturation effects in concentrated systems. At the same time, the incoming X-ray probe of 60–280 eV does not penetrate deep enough and still mostly surface is probed with fluorescence yield XAS. With XRS, one is able to measure more bulk-like properties of light elements [11]. There are a few dedicated XRS setups in the world, where I would like to mention a setup at the European Synchrotron Radiation Facility (ESRF) [17, 18] and another setup at the Stanford Synchrotron Radiation Lightsource (SSRL) [19, 20].

As an example, we discuss XRS measurements performed on (nanosized) $LiBH_4$ hydrogen storage materials [21, 22] at the setup of SSRL [19]. For those experiments, the XRS scans were performed using the inverse energy scan technique with a fixed analyzer energy of 6462.20 eV (mode B mentioned in Section 3). The XRS spectra of this example were measured using 25 detector crystals with an average q-vector of 1.3 atomic units, implying essentially pure dipole transitions, while this dedicated XRS setup had many more detector crystals (at that time 40) which may allow as well higher-order transitions [19], see next sections, but for these studies the other detector crystals were covered. The main additional reason besides the issues mentioned at the beginning of this subchapter for performing XRS experiments on these hydrogen storage materials was that the samples need to be under humid-free environment, and with hydrogen release as well as the pressure is rising, measurements with soft X-rays would be difficult. This example showed that it is possible to study the electronic properties of Li, B, and C of bulk and $LiBH_4$-carbon nanocomposites ($LiBH_4$-C) during de-hydrogenation and the first step of re-hydrogenation.

In particular, for nanocomposites, this is important since there are no many techniques, like XRD used on the bulk samples, able to grasp the electronic structure information on such small and often amorphous materials. In addition, XRS was used to study the decomposition of $NaBH_4$–C nanocomposites (shown in the ESI,† Section S10 of Ref [22]). Note that XRS studies on the lithium edge have as well become relevant for other lithium systems [23] and battery applications, *in situ* de- and re-charging [20]. On the other hand, there are other borohydrides

where the B K-edge XRS (and in addition the Mg L-edge XRS) has recently been measured for another possible hydrogen storage material, $Mg(BH_4)_2$ [24].

4.2. Materials under pressure and in the liquid phase

Although the previously mentioned hydrogen storage materials were only under 1 bar of nitrogen/hydrogen, XRS is also applied in studies with even higher pressures to study the effect of it on materials [25], for example, on iron to gain information on the behavior of it in the inner core of earth [26]. In these higher-pressure studies, phonon scattering is often studied with XRS [27, 28] (NIXS or IXS mentioned in the previous section) to study pressure-induced phase transitions and how the phonon spectrum changes. Since XRS is applied in the hard X-ray regime, it is also easier to get electronic structure measures, similar to direct XAS, on liquid phase systems [29, 30].

4.3. Higher-order electronic transitions

In Section 3, it was mentioned that XRS and XAS may give similar results, but with XRS one is as well able to obtain higher-order transitions above the dipole transition. It has been shown in Ref [31] that octupole transitions can be observed in XRS on rare earth phosphates $RePO_4$ with Re = La, Ce, Pr, and Nd. In this respect, XRS might potentially be used in measuring otherwise spectroscopically unavailable excited states or "optically dark states."

4.4. Summary

In summary, XRS has been mostly used for (*in situ*) electronic structure studies on light elements as the alternative to XAS, and there is a strong focus on materials under high-pressure conditions. In general, XRS studies may become important as well for studies on (heterogenous) catalysts under (close to) industrial operation conditions, because of the advantage of the edge with best chemical resolution without the constraints of the soft X-ray regime (vacuum). As well, XRS is used to gain understanding of the momentum space of phonons of materials of interest (which was not covered in this section).

5. RIXS

Resonant X-ray Raman spectroscopy is now more commonly known as RIXS, but other terms such as resonant X-ray fluorescence spectroscopy (RXFS) and resonant X-ray emission spectroscopy (RXES) have also been used in the past. With RIXS, the incoming X-ray photon energy corresponds (or is close) to an X-ray edge in contrast to XRS. The RIXS process is schematically shown with an one-electron scheme in **Figure 3** next to schematically shown XAS and XES process. The first step of the RIXS process is the same as the XAS process. The second transition is emission from some state, and here it is shown as emission from an occupied state. The XES process is similar to that second step. The processes of RIXS are here only shortly described. For more details on (theory of) RIXS one is referred to Refs. [1, 32–35].

However, for RIXS, the excited electron can relax back into the core hole (elastic emission) and in parallel create an additional excitation from the occupied valence into the unoccupied valence with some energy loss related to this valence excitation as opposed to XES: following the X-ray excitation, subsequent X-ray emission may take place (side-note: Auger decay is stronger than emission decay in the soft X-ray regime). There are a few possibilities that the excited electron decays itself (participator decay channel), which may lead to elastic X-ray scattering, but the excited electron could also have traveled over some excited potential energy surface during the core-hole lifetime which may lead to emission to a vibrationally excited state. Another option for the participator channel is that the excited electron decays itself and transfers energy to an electron in the valence band which gets excited into some unoccupied state (e.g., a so-called charge transfer state or a valence-valence excitation). Also an electron from the valence band (spectator decay channel) may decay instead of the excited electron (participator channel). This may lead effectively to the same final situation from this one-electron picture of **Figure 3**.

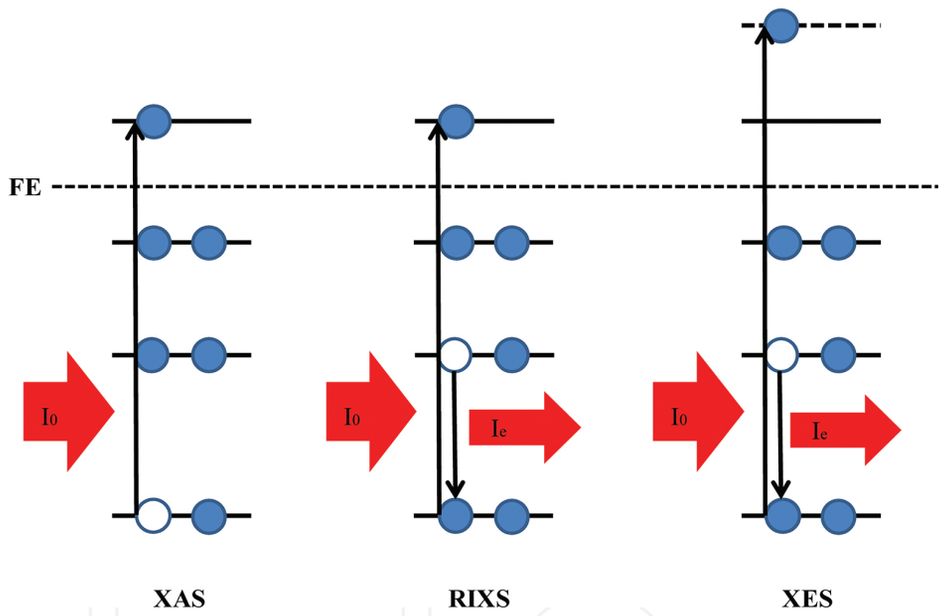

Figure 3. Schematic representation of the different core spectroscopies: X-ray absorption spectroscopy (XAS), resonant inelastic X-ray scattering (RIXS), and (nonresonant) X-ray emission spectroscopy (XES). FE indicated the Fermi level. Solid horizontal lines indicate unoccupied states within the system, while the dotted line indicates a virtual state for electrons ("free electrons"). Red lines indicate incident and emitted radiation.

So, **Figure 3** showed the XAS, XES, and RIXS processes by single-electron movements. However, one should think about these processes in total energy terms. The case for the combination of XAS, RIXS, and XES is shown in **Figure 4**.

As simplified above, RIXS is a combination of XAS (the absorption of the photon) and XES (the emission of a photon), and **Figure 4** shows that with RIXS it is then possible to reach excited states of the material. Here it is not stressed what kind of excited states these are, since this can be any type of excited state. That means that with RIXS (and sufficient resolution in the emission spectrometer) one can obtain information on electronic excited states (e.g., dd

excitations in 3d-materials) but as well on vibrationally and magnetically excited states [36]. The figure does not show energy gains (anti-Stokes Raman), but in principle this is possible if the system before the X-ray excitation is already in an excited state.

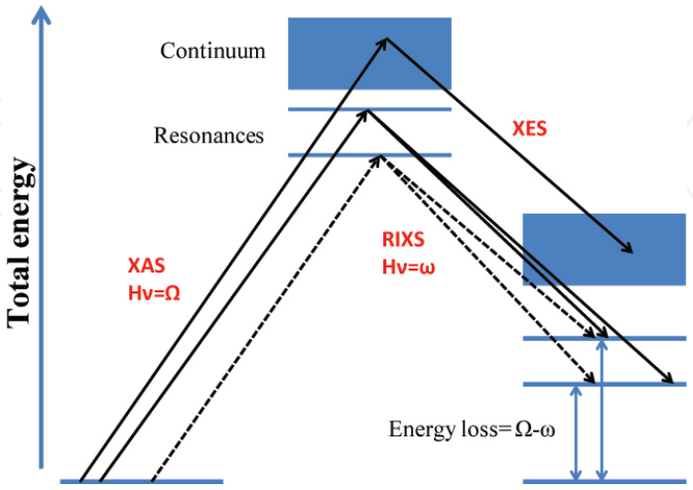

Figure 4. Total energy scheme of the processes of X-ray absorption (XAS), X-ray emission (XES) and resonant inelastic X-ray scattering (RIXS) with X-ray absorption resonances and the continuum as possible excitation channels (intermediate state for RIXS/XES) and final states for RIXS at different energy (energy loss) than the original ground state.

In the earlier days of RIXS, Butorin showed advantages of the RIXS technique, such as clear band showing allowed dd excitations compared to EELS and UV-VIS absorption spectra where dd transitions often appear as weak structures [37]. RIXS spectroscopy gained increased interest with the advances on the brilliance of synchrotrons and X-ray free-electron lasers as well as advances in more efficient detectors. More information on RIXS and its capabilities can be found in Refs. [5, 38, 39].

6. Some applications of RIXS

6.1. Soft X-ray RIXS on cuprates

In the early days, soft X-ray RIXS with moderate resolution was performed a lot on standard compounds such as manganese oxide (MnO) [37, 40], cobalt oxide (CoO) [40], and nickel oxide (NiO) [40–43]. Interestingly, in the soft X-ray regime when the SAXES spectrometer [44] became available with a much better energy resolution, and the general improved resolution was established on MnO [45], CoO [46], and NiO [47], high-energy resolution RIXS was focused mostly on the Cu L-edge of high-temperature superconductors (HT-SC) and representative HT-SC model compounds and as well with some measurements at the oxygen K-edge to gain understanding of superconducting properties related to phonon, magnon, and electronic structure, for example, Refs [48–52] for Cu L-edge and Refs. [53, 54] for the oxygen K-edge RIXS of HT-SC (model) compounds.

Nowadays, with more high-resolution RIXS spectrometers becoming available with even advanced features [55], high-resolution soft X-ray RIXS studies toward other 3d- (e.g., iron selenides, manganites, nickelates, or cobalt), 4d-, and 5d-metal (e.g., iridium) materials and to 4f-materials are expected for investigations into solid-state applications like superconductivity (FeSe-related), multiferroics, topological insulators, etc.

6.2. RIXS on metal organics – hard X-ray RIXS: 1s2p and 1s3p RIXS

In general, organic materials suffer from the X-ray probe, for example, the X-rays create beam damage. Hard X-rays have a lower cross section with metallic components in metal organics, such as proteins and homogeneous metal-containing catalysts than soft X-rays. In order to decrease the chances of beam damage, hard X-ray RIXS is often applied on these biologically/homogeneous catalysis relevant materials, especially focusing on properties concerning the active metal center of these systems.

In line with XRS, hard X-ray RIXS can also be used to study the edges with best chemical resolution indirectly [56, 57]. For example, for iron one can excite the (pre-)K-edge (1s core hole with excitation into the 3d-shell-related states) and probe the Ka (2p emission) or Kb (3p) emission. In these cases, the final state of the RIXS process is similar to the normal 2p XAS or 3p XAS (a hole in the 2p/3p and an additional electron in 3d). The emission resembles then the normal 2p (3p) XAS measured in the soft X-ray regime, but the spectrum measured via 1s2p (1s3p) RIXS may have additional features [58] due to quadrupole and monopole contributions, since with RIXS as a two-photon process the dipole selection rule has to be twice taken into account.

6.3. RIXS on simple semiconductors: electron-phonon coupling, band gap properties

In the hard X-ray regime, RIXS has been applied as well to study electron-phonon interactions of cuprates by focusing on the phonon progression [59], and in essence, the same technique can be performed in soft X-ray RIXS with high-energy resolution as long as there are not too many different phonon modes interfering. In the soft X-ray regime, electron-phonon scattering properties have been analyzed by measuring both RIXS and X-ray emission spectroscopy (XES) with a relatively low-energy resolution RIXS spectrometer [60] compared to the current standard as function of temperature for silicon and silicon carbide.

Resonant inelastic X-ray scattering and X-ray emission are very often applied in a similar fashion. Above certain energies, for example, well above the X-ray resonances, in the ionization regime, when one observes emitted X-ray photons, one speaks simply of *normal* XES.

By applying the combination of RIXS and XES, one could get (relative) measures on the angular and crystal momentum transfer due to electron-phonon scattering. This gives you an average electron-phonon scattering picture, so it is perfectly fine if there are many phonon modes. Comparing the different results on these compounds, a form of silicon carbide (6H-SiC) showed a much stronger electron-phonon scattering effect than pure silicon for both crystal momentum transfer and angular momentum transfer [61, 62]. In **Figure 5**, comparison of calculated silicon partial density of states (DOS) of 6H-SiC with the difference in XES as

function of temperature with reference to room temperature is given. One sees that as function of temperature, the XES difference shows a decrease related to s-DOS and an increase related to p-DOS, while the core hole is of 2p character. In general, s-(and d-)DOS is expected in the XES with a Si 2p core hole and the increase in p-DOS with temperature is therefore a measure for the amount of angular momentum transfer events in the core-hole lifetime.

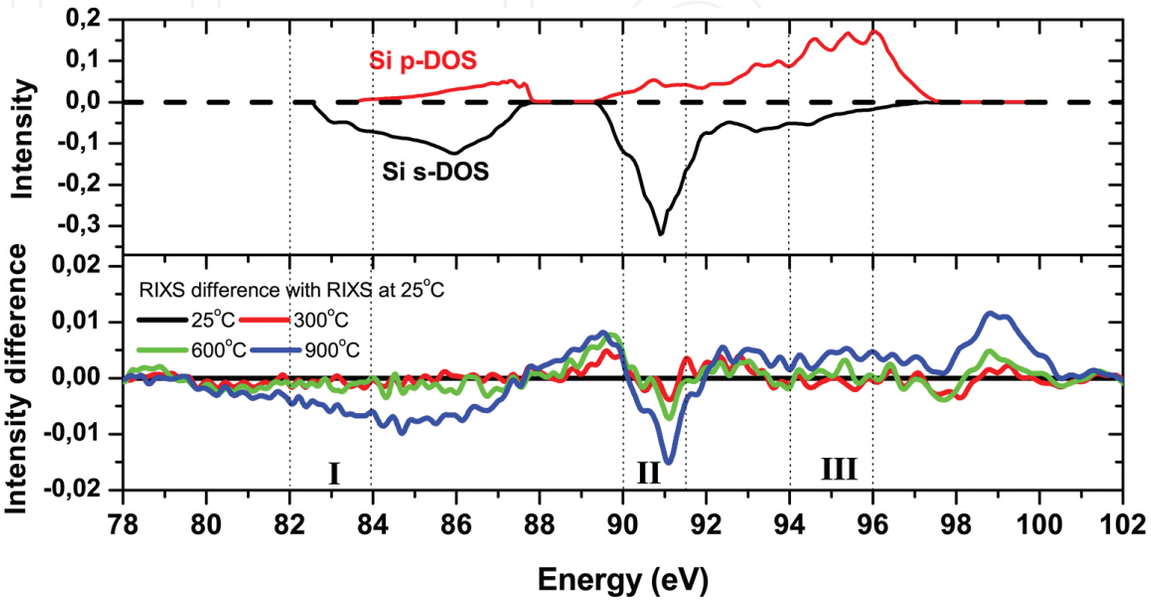

Figure 5. Top: calculated Si s-DOS and p-DOS for silicon carbide (6H-SiC). Bottom: difference in the XES with the XES at room temperature for 6H-SiC. This figure was adapted from Ref. [62] and is taken with permission.

For insulators and semiconductors, the first electronic energy loss observed in RIXS is directly related to the (element-specific) band gap, and by combining the information of RIXS with XAS and XES, one is able to identify the valence and conduction band behavior as a function of temperature [63, 64], which is important to know for semiconductor applications under extreme temperature conditions.

6.4. RIXS on liquids and on ions and organic molecules solved in liquid

In general, liquids at synchrotrons are measured by flow cells or liquid jets. For hard X-ray RIXS measurements, there are in principal no side conditions, but for soft X-ray RIXS measurements, you need to stay below a certain pressure in order to still be able to get X-rays on the liquid and to measure the emitted X-rays. There are a few setups in the world that can perform these measurements routinely, for example, the setups explained in Refs. [6, 65]. For liquids, the soft X-ray regime of RIXS [66, 67] is more important because often you want to study resonantly the oxygen K-edge and nitrogen K-edges which are at about 500 and 400 eV in the soft X-ray regime, respectively. Liquid jet RIXS with relatively low-energy resolution (~500 meV) has now, for example, been successfully employed on liquid and gas phase water [68, 69], methanol and other alcohols [70], 3d-metal ions solved in water, for example, Mn^{2+} (and Mn^{2+} organic complexes) [71] and Ni^{2+} in water [72], $Fe(CO)_5$ solved in ethanol [73, 74],

$Fe(CN)_6$ solved in water [74–76], 2-mercaptopyridine solved in water [77] and (models for) biologically relevant proteins in solution [71, 78–80].

As an example of RIXS on liquids, **Figure 6** shows the oxygen K-edge RIXS on resonance and far above the resonance (nonresonant X-ray emission) for methanol, ethanol, propanol, butanol, pentanol, and hexanol. It shows the main double-peak structure for all these alcohols, where the interpretation of this double-peak structure has been under debate for oxygen K-edge of water. As explained by Schreck et al., the relative ratio of this main double-peak structure corresponds to the amount of hydrogen bonds (expected from simulations) [70].

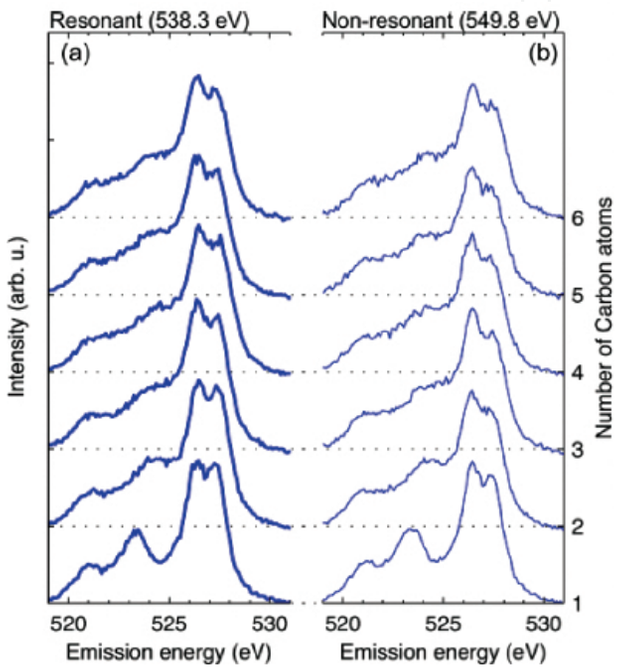

Figure 6. From top to bottom: oxygen K-edge on resonance (a) and oxygen K-edge nonresonant X-ray emission (b) of liquid hexanol, pentanol, butanol, propanol, ethanol and methanol. Figure taken from Ref. [70].

For the more sophisticated RIXS spectrometers with high resolution (~50 meV), flow cells are preferred in order to keep good vacuum conditions in the overall vacuum chamber and in the spectrometer. With the first high-resolution RIXS spectrometer available at the Swiss Light Source [44, 81], RIXS with vibrational-resolved resolution was acquired and analyzed for water [68] and acetone and the acetone-chloroform complex [82], and for the latter, two systems ground state potential energy surfaces could be reconstructed from the vibrational progression observed with vibrationally resolved RIXS.

By combining pump-laser probe-X-ray photons, one can get time-resolved information on materials. In this case, it is possible that the pump-laser excites the material to some excited state and the probe X-ray followed by X-ray scattering may lead to anti-stokes RIXS features (that is features observed at X-ray emission energies higher than the probe X-ray excitation energy). The first indications have been shown in X-ray free-electron laser experiments on $Fe(CO)_5$ solved in ethanol [74].

7. Summary

A short overview of X-ray Raman spectroscopy and resonant X-ray Raman spectroscopy (RIXS) has been given with special attention to what these element-specific spectroscopies can contribute to a better understanding of materials, or in other words how chemistry might benefit from Raman spectroscopy studies in the X-ray regime. Here it was shown that XRS and RIXS can supply information on (local, occupied, and unoccupied valence) electronic structure relevant to chemical activity, as well as supplying data to coupling of electronic structure with vibrational (electron-phonon interaction) and spin structure (electron-magnon interaction). In addition, with X-ray FELs, XRS and RIXS can be applied to (optically) excited states, and in particular the shift of these spectroscopies from synchrotrons to X-ray free-electron lasers [83] may become an important transition for time-dependent electronic and phononic structure studies. As well, (future) diffraction-limited storage rings will enhance the energy resolution for XRS and RIXS [84].

Author details

Piter Sybren Miedema

Address all correspondence to: p.s.miedema@gmail.com

Institute of Methods and Instrumentation for Synchrotron Radiation Research (FG-ISRR), Helmholtz-Zentrum Berlin, Germany

References

[1] F. de Groot and A. Kotani, Core Level Spectroscopy of Solids. CRC Press, Boca Raton, Florida, 2008

[2] L. A. Grunes, "Study of the K edges of 3d transition metals in pure and oxide form by X-ray absorption spectroscopy," *Phys. Rev. B*, vol. 27, no. 4, pp. 2111–2131, 1983.

[3] P.S. Miedema, "X-ray Spectroscopy of Inorganic Materials," PhD thesis, Utrecht University, Utrecht, The Netherlands, 2012.

[4] G. van der Laan and A. I. Figueroa, "X-ray magnetic circular dichroism—A versatile tool to study magnetism," *Coord. Chem. Rev.*, vol. 277–278, pp. 95–129, Mar. 2014.

[5] F. J. Himpsel, "Photon-in photon-out soft X-ray spectroscopy for materials science," *Phys. Stat. Sol.*, vol. 248, no. 2, pp. 292–298, Feb. 2011.

[6] K. Kunnus, I. Rajkovic, S. Schreck, W. Quevedo, S. Eckert, M. Beye, E. Suljoti, C. Weniger, C. Kalus, S. Grübel, M. Scholz, D. Nordlund, W. Zhang, R. W. Hartsock, K. J.

Gaffney, W. F. Schlotter, J. J. Turner, B. Kennedy, F. Hennies, S. Techert, P. Wernet, A. Föhlisch, "A setup for resonant inelastic soft X-ray scattering on liquids at free electron laser light sources.," *Rev. Sci. Instrum.*, vol. 83, no. 12, p. 123109, Dec. 2012.

[7] P. S. Miedema, M. M. van Schooneveld, R. Bogerd, T. C. R. Rocha, M. Hävecker, A. Knop-Gericke, F. M. F. de Groot, "Oxygen binding to cobalt and iron phthalocyanines as determined from in situ x-ray absorption spectroscopy," *J. Phys. Chem. C*, vol. 115, no. 51, pp. 25422–25428, Dec. 2011.

[8] H. Bluhm, "Photoelectron spectroscopy of surfaces under humid conditions," *J. Electron Spectrosc. Relat. Phenom.*, vol. 177, no. 2–3, pp. 71–84, 2010.

[9] M. Hävecker, T. Schedel-niedrig, R. Schlögl, I. Chemistry, F. Mpg, "High-pressure low-energy XAS: a new tool for probing reacting surfaces of heterogeneous catalysts," *Top. Catal.*, vol. 10, pp. 187–198, 2000.

[10] J. J. Velasco-Vélez, V. Pfeifer, M. Hävecker, R. Wang, A. Centeno, A. Zurutuza, G. Algara-Siller, E. Stotz, K. Skorupska, D. Teschner, P. Kube, P. Braeuninger-Weimer, S. Hofmann, R. Schlögl, A. Knop-Gericke, "Atmospheric pressure X-ray photoelectron spectroscopy apparatus: bridging the pressure gap," *Rev. Sci. Instrum.*, vol. 87, p. 053121, 2016.

[11] U. Bergmann, P. Glatzel, S. P. Cramer, "Bulk-sensitive XAS characterization of light elements: from X-ray Raman scattering to X-ray Raman spectroscopy," *Microchem. J.*, vol. 71, no. 2–3, pp. 221–230, Apr. 2002.

[12] R. Alonso-Mori, J. Kern, D. Sokaras, T. C. Weng, D. Nordlund, R. Tran, P. Montanez, J. Delor, V. K. Yachandra, J. Yano, U. Bergmann, "A multi-crystal wavelength dispersive X-ray spectrometer," *Rev. Sci. Instrum.*, vol. 83, p. 073114, 2012.

[13] E. Burkel, "Phonon spectroscopy by inelastic X-ray scattering," *Rep. Prog. Phys.*, vol. 63, no. 2, pp. 171–232, Feb. 2000.

[14] F. Sette, M. H. Krisch, C. Masciovecchio, G. Ruocco, G. Monaco, "Dynamics of glasses and glass-forming liquids studied by inelastic X-ray scattering," *Science (80-.).*, vol. 280, no. 5369, pp. 1550–1555, 1998.

[15] O. Chubar, G. Geloni, V. Kocharyan, A. Madsen, E. Saldin, S. Serkez, Y. Shvyd'ko, J. Sutter, "Ultra-high-resolution inelastic X-ray scattering at high-repetition-rate self-seeded X-ray free-electron lasers," *J. Synchrotron Radiat.*, vol. 23, no. 2, pp. 410–424, 2016.

[16] A. Q. R. Baron, Y. Tanaka, D. Miwa, D. Ishikawa, T. Mochizuki, K. Takeshita, S. Goto, T. Matsushita, H. Kimura, F. Yamamoto, T. Ishikawa, "Early commissioning of the SPring-8 beamline for high resolution inelastic X-ray scattering," *Nucl. Instrum. Methods Phys. Res. A Accel. Spectrom., Detect. Assoc. Equip.*, vol. 467–468, pp. 627–630, 2001.

[17] S. Huotari, G. Vankó, F. Albergamo, C. Ponchut, H. Graafsma, C. Henriquet, R. Verbeni, G. Monaco, "Improving the performance of high-resolution X-ray spectrometers with position-sensitive pixel detectors," *J. Synchrotron Radiat.*, vol. 12, pp. 467–472, 2005.

[18] S. Huotari, F. Albergamo, G. Vankó, R. Verbeni, G. Monaco, "Resonant inelastic hard X-ray scattering with diced analyzer crystals and position-sensitive detectors," *Rev. Sci. Instrum*., vol. 77, p. 053102, 2006.

[19] D. Sokaras, D. Nordlund, T. C. Weng, R. A. Mori, P. Velikov, D. Wenger, A. Garachtchenko, M. George, V. Borzenets, B. Johnson, Q. Qian, T. Rabedeau, U. Bergmann, "A high resolution and large solid angle X-ray Raman spectroscopy end-station at the Stanford Synchrotron Radiation Lightsource," *Rev. Sci. Instrum*., vol. 83, p. 043112, 2012.

[20] A. Braun, D. Nordlund, S. W. Song, T. W. Huang, D. Sokaras, X. Liu, W. Yang, T. C. Weng, Z. Liu, "Hard X-rays in-soft X-rays out: an operando piggyback view deep into a charging lithium ion battery with X-ray Raman spectroscopy," *J. Electron Spectrosc. Relat. Phenom*., vol. 200, pp. 257–263, 2015.

[21] P. S. Miedema, P. Ngene, A. M. J. van der Eerden, T.-C. Weng, D. Nordlund, D. Sokaras, R. Alonso-Mori, A. Juhin, P. E. de Jongh, F. M. F. de Groot, "In situ X-ray Raman spectroscopy of $LiBH_4$," *Phys. Chem. Chem. Phys*., vol. 14, no. 16, pp. 5581–7, Apr. 2012.

[22] P. S. Miedema, P. Ngene, A. M. J. van der Eerden, D. Sokaras, T.-C. Weng, D. Nordlund, Y. S. Au, F. M. F. de Groot, "In situ X-ray Raman spectroscopy study of the hydrogen sorption properties of lithium borohydride nanocomposites.," *Phys. Chem. Chem. Phys*., vol. 16, no. 41, pp. 22651–22658, Oct. 2014.

[23] T. A. Pascal, U. Boesenberg, R. Kostecki, T. J. Richardson, T. C. Weng, D. Sokaras, D. Nordlund, E. McDermott, A. Moewes, J. Cabana, D. Prendergast, "Finite temperature effects on the X-ray absorption spectra of lithium compounds: first-principles interpretation of X-ray Raman measurements," *J. Chem. Phys*., vol. 140, p. 034107, 2014.

[24] C. J. Sahle, S. Kujawski, A. Remhof, Y. Yan, N. Stadie, A. Al-Zein, M. Tolan, S. Huotari, M. Krisch, C. Sternemann, "*In-situ* characterization of the decomposition behavior of $Mg(BH_4)_2$ by X-ray Raman scattering spectroscopy," *Phys. Chem. Chem. Phys*., vol. 18, pp. 5397–5403, 2016.

[25] J. P. Rueff, A. Shukla, "Inelastic X-ray scattering by electronic excitations under high pressure," *Rev. Mod. Phys*., vol. 82, pp. 847–896, 2010.

[26] A. Nyrow, J. S. Tse, N. Hiraoka, S. Desgreniers, T. Büning, K. Mende, M. Tolan, M. Wilke, C. Sternemann, "Pressure induced spin transition revealed by iron M2,3-edge spectroscopy," *Appl. Phys. Lett*., vol. 104, no. 26, p. 262408, Jun. 2014.

[27] V. M. Giordano, M. Krisch, G. Monaco, "Phonon spectroscopy at high pressure by inelastic X-ray scattering," *J. Synchrotron Radiat*., vol. 16, pp. 707–713, 2009.

[28] M. Krisch, "Status of phonon studies at high pressure by inelastic X-ray scattering," *J. Raman Spectrosc*., vol. 34, no. 7–8, pp. 628–632, 2003.

[29] J. Niskanen, C. J. Sahle, I. Juurinen, J. Koskelo, S. Lehtola, R. Verbeni, H. Müller, M. Hakala, S. Huotari, "Protonation dynamics and hydrogen bonding in aqueous sulfuric acid," J. Phys. Chem. B, vol. 119. pp. 11732–11739, 2015.

[30] C. J. Sahle, M. a Schroer, I. Juurinen, J. Niskanen, "Influence of TMAO and urea on the structure of water studied by inelastic X-ray scattering.," *Phys. Chem. Chem. Phys.*, vol. 18, pp. 16518–16526, 2016.

[31] S. Huotari, E. Suljoti, C. J. Sahle, S. Rädel, G. Monaco, F. M. F. De Groot, "High-resolution nonresonant X-ray Raman scattering study on rare earth phosphate nanoparticles," *New J. Phys.*, vol. 17, p. 043041, 2015.

[32] A. Kotani and S. Shin, "Resonant inelastic X-ray scattering spectra for electrons in solids," *Rev. Mod. Phys.*, vol. 73, no. January, pp. 203–246, 2001.

[33] L. J. P. Ament, M. van Veenendaal, T. P. Devereaux, J. P. Hill, J. van den Brink, "Resonant inelastic X-ray scattering studies of elementary excitations," *Rev. Mod. Phys.*, vol. 83, no. 2, pp. 705–767, Jun. 2011.

[34] P. Glatzel, M. Sikora, G. Smolentsev, M. Fernández-García, "Hard X-ray photon-in photon-out spectroscopy," *Catal. Today*, vol. 145, pp. 294–299, 2009.

[35] F. Gel'mukhanov, H. Agren, "Resonant X-ray Raman scattering," *Phys. Rep.*, vol. 312, pp. 87–330, 1999.

[36] S. Fatale, S. Moser, M. Grioni, "Magnetic excitations in soft X-ray RIXS: recent developments," *J. Electron Spectrosc. Relat. Phenom.*, vol. 200, pp. 274–281, 2015.

[37] S. Butorin, J.-H. Guo, M. Magnuson, P. Kuiper, J. Nordgren, "Low-energy d-d excitations in MnO studied by resonant X-ray fluorescence spectroscopy," *Phys. Rev. B*, vol. 54, no. 7, pp. 4405–4408, 1996.

[38] A. Kotani, "Resonant inelastic X-ray scattering in d and f electron systems," *Eur. Phys. J. B*, vol. 47, no. 1, pp. 3–27, Sep. 2005.

[39] P. Glatzel, T.-C. Weng, K. Kvashnina, J. Swarbrick, M. Sikora, E. Gallo, N. Smolentsev, R. A. Mori, "Reflections on hard X-ray photon-in/photon-out spectroscopy for electronic structure studies," *J. Electron Spectrosc. Relat. Phenom.*, vol. 188, pp. 17–25, Jun. 2013.

[40] S. M. Butorin, "Resonant inelastic X-ray scattering as a probe of optical scale excitations in strongly electron-correlated systems: quasi-localized view," *J. Electron Spectrosc. Relat. Phenom.*, vol. 110–111, pp. 213–233, Oct. 2000.

[41] M. Magnuson, S. M. Butorin, A. Agui, J. Nordgren, "Resonant soft X-ray Raman scattering of NiO," *J. Phys. Condens. Matter*, vol. 14, pp. 3669–3676, 2002.

[42] L. Braicovich, C. Dallera, G. Ghiringhelli, N. B. Brookes, J. B. Goedkoop, M. A. Van Veenendaal, "X-ray L2,3 resonant Raman scattering from NiO: spin flip and intermediate-state relaxation," *Phys. Rev. B*, vol. 55, no. 24, pp. 989–992, 1997.

[43] H. Ishii, Y. Ishiwata, R. Eguchi, Y. Harada, M. Watanabe, A. Chainani, S. Shin, "Resonant soft X-ray emission spectroscopy of NiO across the Ni L2,3 thresholds," *J. Phys. Soc. Jpn.*, vol. 70, no. 6, pp. 1813–1816, 2001.

[44] G. Ghiringhelli, A. Piazzalunga, C. Dallera, G. Trezzi, L. Braicovich, T. Schmitt, V. N. Strocov, R. Betemps, L. Patthey, X. Wang, M. Grioni, "SAXES, a high resolution spectrometer for resonant X-ray emission in the 400-1600 eV energy range," *Rev. Sci. Instrum.*, vol. 77, p. 113108, 2006.

[45] G. Ghiringhelli, M. Matsubara, C. Dallera, F. Fracassi, A. Tagliaferri, N. B. Brookes, A. Kotani, L. Braicovich, "Resonant inelastic X-ray scattering of MnO◎: L 2, 3 edge measurements and assessment of their interpretation," *Phys. Rev. B*, vol. 73, pp. 8–11, 2006.

[46] S. Chiuzbăian, T. Schmitt, M. Matsubara, A. Kotani, G. Ghiringhelli, C. Dallera, A. Tagliaferri, L. Braicovich, V. Scagnoli, N. Brookes, U. Staub, L. Patthey, "Combining M- and L-edge resonant inelastic X-ray scattering for studies of 3d transition metal compounds," *Phys. Rev. B*, vol. 78, no. 24, p. 245102, Dec. 2008.

[47] G. Ghiringhelli, M. Matsubara, C. Dallera, F. Fracassi, R. Gusmeroli, A. Piazzalunga, A. Tagliaferri, N. B. Brookes, A. Kotani, L. Braicovich, "NiO as a test case for high resolution resonant inelastic soft X-ray scattering," *J. Phys. Condens. Matter*, vol. 17, no. 35, pp. 5397–5412, Sep. 2005.

[48] L. Braicovich, M. Moretti Sala, L. J. P. Ament, V. Bisogni, M. Minola, G. Balestrino, D. Di Castro, G. M. De Luca, M. Salluzzo, G. Ghiringhelli, J. Van Den Brink, "Momentum and polarization dependence of single-magnon spectral weight for Cu L3-edge resonant inelastic X-ray scattering from layered cuprates," *Phys. Rev. B*, vol. 81, p. 174533, 2010.

[49] L. Braicovich, J. van den Brink, V. Bisogni, M. M. Sala, L. J. P. Ament, N. B. Brookes, G. M. De Luca, M. Salluzzo, T. Schmitt, V. N. Strocov, G. Ghiringhelli, "Magnetic excitations and phase separation in the underdoped La_{2-x}Sr_{x}CuO_{4} superconductor measured by resonant inelastic X-ray scattering," *Phys. Rev. Lett.*, vol. 104, no. 7, p. 077002, Feb. 2010.

[50] L. Braicovich, L. J. P. Ament, V. Bisogni, F. Forte, C. Aruta, G. Balestrino, N. B. Brookes, G. M. De Luca, P. G. Medaglia, F. M. Granozio, M. Radovic, M. Salluzzo, J. Van Den Brink, G. Ghiringhelli, "Dispersion of magnetic excitations in the cuprate La_2CuO_4 and $CaCuO_2$ compounds measured using resonant X-ray scattering," *Phys. Rev. Lett.*, vol. 102, no. 16, pp. 22–25, 2009.

[51] C. Monney, V. Bisogni, K.-J. Zhou, R. Kraus, V. N. Strocov, G. Behr, J. Málek, R. Kuzian, S.-L. Drechsler, S. Johnston, A. Revcolevschi, B. Büchner, H. M. Rønnow, J. van den Brink, J. Geck, T. Schmitt, "Determining the short-range spin correlations in the spin-chain Li_2CuO_2 and $CuGeO_3$ compounds using resonant inelastic X-ray scattering," *Phys. Rev. Lett.*, vol. 110, no. 8, p. 087403, 2013.

[52] C. Monney, T. Schmitt, C. E. Matt, J. Mesot, V. N. Strocov, O. J. Lipscombe, S. M. Hayden, J. Chang, "Resonant inelastic X-ray scattering study of the spin and charge excitations in the overdoped superconductor $La_{1.77}Sr_{0.23}CuO_4$," *Phys. Rev. B*, vol. 93, no. 7, p. 075103, 2016.

[53] B. Freelon, A. Augustsson, J. H. Guo, P. G. Medaglia, A. Tebano, G. Balestrino, C. L. Dong, C. L. Chang, P. a. Glans, T. Learmonth, K. E. Smith, J. Nordgren, Z. Hussain, "Low energy electronic spectroscopy of an infinite-layer cuprate: a resonant inelastic X-ray scattering study of $CaCuO_2$," *Phys. C*, vol. 470, no. 3, pp. 187–192, 2010.

[54] C. C. Chen, M. Sentef, Y. F. Kung, C. J. Jia, R. Thomale, B. Moritz, a. P. Kampf, T. P. Devereaux, "Doping evolution of the oxygen K-edge X-ray absorption spectra of cuprate superconductors using a three-orbital Hubbard model," *Phys. Rev. B*, vol. 87, p. 165144, 2013.

[55] L. Braicovich, M. Minola, G. Dellea, M. Le Tacon, M. Moretti Sala, C. Morawe, J. C. Peffen, R. Supruangnet, F. Yakhou, G. Ghiringhelli, N. B. Brookes, "The simultaneous measurement of energy and linear polarization of the scattered radiation in resonant inelastic soft X-ray scattering, " *Rev. Sci. Instrum.*, vol. 85, no. 11, pp. 115104, 2014.

[56] F. M. F. de Groot, P. Glatzel, U. Bergmann, P. a van Aken, R. a Barrea, S. Klemme, M. Hävecker, A. Knop-Gericke, W. M. Heijboer, B. M. Weckhuysen, "1s2p resonant inelastic X-ray scattering of iron oxides.," *J. Phys. Chem. B*, vol. 109, no. 44, pp. 20751–20762, Nov. 2005.

[57] M. Lundberg, T. Kroll, S. DeBeer, U. Bergmann, S. A Wilson, P. Glatzel, D. Nordlund, B. Hedman, K. O. Hodgson, E. I. Solomon, "Metal-ligand covalency of iron complexes from high-resolution resonant inelastic X-ray scattering.," *J. Am. Chem. Soc.*, vol. 135, no. 45, pp. 17121–17134, Nov. 2013.

[58] T. Kroll, R. G. Hadt, S. A. Wilson, M. Lundberg, J. J. Yan, T. C. Weng, D. Sokaras, R. Alonso-Mori, D. Casa, M. H. Upton, B. Hedman, K. O. Hodgson, E. I. Solomon, "Resonant inelastic X-ray scattering on ferrous and ferric bis-imidazole porphyrin and cytochrome c: nature and role of the axial methionine-fe bond," *J. Am. Chem. Soc.*, vol. 136, no. 52, pp. 18087–18099, 2014.

[59] H. Yavaş, M. van Veenendaal, J. van den Brink, L. J. P. Ament, A. Alatas, B. M. Leu, M.-O. Apostu, N. Wizent, G. Behr, W. Sturhahn, H. Sinn, E. E. Alp, "Observation of phonons with resonant inelastic X-ray scattering.," *J. Phys. Condens. Matter*, vol. 22, p. 485601, 2010.

[60] J. Nordgren, G. Bray, S. Cramm, R. Nyholm, J.-E. Rubensson, N. Wassdahl, "Soft X-ray emission spectroscopy using monochromatized synchrotron radiation (invited)," *Rev. Sci. Instrum.*, vol. 60, no. 7, p. 1690, 1989.

[61] M. Beye, F. Hennies, M. Deppe, E. Suljoti, M. Nagasono, W. Wurth, A. Föhlisch, "Dynamics of electron-phonon scattering: crystal- and angular-momentum transfer probed by resonant inelastic X-ray scattering," *Phys. Rev. Lett.*, vol. 103, no. 23, p. 237401, Dec. 2009.

[62] P. S. Miedema, M. Beye, R. Könnecke, G. Schiwietz, A. Föhlisch, "The angular- and crystal-momentum transfer through electron–phonon coupling in silicon and silicon-carbide: similarities and differences," *New J. Phys.*, vol. 16, no. 9, p. 093056, Sep. 2014.

[63] M. Beye, F. Hennies, M. Deppe, E. Suljoti, M. Nagasono, W. Wurth, A. Föhlisch, "Measurement of the predicted asymmetric closing behaviour of the band gap of silicon using X-ray absorption and emission spectroscopy," *New J. Phys*., vol. 12, no. 4, p. 043011, Apr. 2010.

[64] P. S. Miedema, M. Beye, R. Könnecke, G. Schiwietz, A. Föhlisch, "Thermal evolution of the band edges of 6H-SiC: X-ray methods compared to the optical band gap," *J. Electron Spectrosc. Relat. Phenom*., vol. 197, pp. 37–42, Dec. 2014.

[65] L. Weinhardt, M. Blum, O. Fuchs, A. Benkert, F. Meyer, M. Bär, J. D. Denlinger, W. Yang, F. Reinert, C. Heske, "RIXS investigations of liquids, solutions, and liquid/solid interfaces," *J. Electron Spectrosc. Relat. Phenom*., vol. 188, pp. 111–120, Jun. 2013.

[66] J. E. Rubensson, F. Hennies, A. Pietzsch, "High-resolution resonant inelastic soft X-ray scattering applied to liquids," *J. Electron Spectrosc. Relat. Phenom*., vol. 188, pp. 79–83, 2013.

[67] J.-E. Rubensson, "Resonant inelastic soft X-ray scattering applied to molecular materials," *J. Electron Spectrosc. Relat. Phenom*., vol. 200, pp. 239–246, 2015.

[68] A. Pietzsch, F. Hennies, P. S. Miedema, B. Kennedy, J. Schlappa, T. Schmitt, V. N. Strocov, A. Föhlisch, "Snapshots of the fluctuating hydrogen bond network in liquid water on the sub-femtosecond timescale with vibrational resonant inelastic X-ray scattering," *Phys. Rev. Lett*., vol. 114, p. 088302, 2015.

[69] L. Weinhardt, A. Benkert, F. Meyer, M. Blum, R. G. Wilks, W. Yang, M. Bär, F. Reinert, C. Heske, "Nuclear dynamics and spectator effects in resonant inelastic soft X-ray scattering of gas-phase water molecules," *J. Chem. Phys*., vol. 136, no. 14, 2012.

[70] S. Schreck, A. Pietzsch, K. Kunnus, B. Kennedy, W. Quevedo, P. S. Miedema, P. Wernet, A. Föhlisch, "Dynamics of the OH group and the electronic structure of liquid alcohols," *Struct. Dyn*., vol. 1, no. 5, p. 054901, Sep. 2014.

[71] S. I. Bokarev, M. Khan, M. K. Abdel-Latif, J. Xiao, R. Hilal, S. G. Aziz, E. F. Aziz, O. Kühn, "Unraveling the electronic structure of photocatalytic manganese complexes by L-Edge X-ray spectroscopy," *J. Phys. Chem. C*, vol. 119, no. 33, pp. 19192–19200, 2015.

[72] K. Kunnus, I. Josefsson, S. Schreck, W. Quevedo, P. S. Miedema, S. Techert, F. M. F. de Groot, M. Odelius, P. Wernet, A. Föhlisch, "From ligand fields to molecular orbitals: probing the local valence electronic structure of Ni(2+) in aqueous solution with resonant inelastic X-ray scattering.," *J. Phys. Chem. B*, vol. 117, no. 51, pp. 16512–16521, Dec. 2013.

[73] P. Wernet, K. Kunnus, I. Josefsson, I. Rajkovic, W. Quevedo, M. Beye, S. Schreck, S. Grübel, M. Scholz, D. Nordlund, W. Zhang, R. W. Hartsock, W. F. Schlotter, J. J. Turner, B. Kennedy, F. Hennies, F. M. F. de Groot, K. J. Gaffney, S. Techert, M. Odelius, A. Föhlisch, "Orbital-specific mapping of the ligand exchange dynamics of Fe(CO)5 in solution," *Nature*, vol. 520, pp. 78–81, 2015.

[74] K. Kunnus, "Probing dynamic pathways and electronic structure of coordination complexes with soft X-ray spectroscopy," Universität Potsdam, 2014.

[75] N. Engel, S. I. Bokarev, E. Suljoti, R. Garcia-Diez, K. M. Lange, K. Atak, R. Golnak, A. Kothe, M. Dantz, O. Kühn, E. F. Aziz, "Chemical bonding in aqueous ferrocyanide: experimental and theoretical X-ray spectroscopic study," *J. Phys. Chem. B*, vol. 118, no. 6, pp. 1555–1563, 2014.

[76] K. Kunnus, W. Zhang, M. G. Delcey, R. V Pinjari, P. S. Miedema, S. Schreck, W. Quevedo, H. Schroeder, A. Föhlisch, K. J. Gaffney, M. Lundberg, M. Odelius, P. Wernet, "Viewing the valence electronic structure of ferric and ferrous hexacyanide in solution from the Fe and cyanide perspectives," *J. Phys. Chem. B*, vol. 120, pp. 7182–7194, 2016.

[77] S. Eckert, P. S. Miedema, W. Quevedo, B. O'Cinneide, M. Fondell, M. Beye, A. Pietzsch, M. Ross, M. Khalil, A. Föhlisch, "Molecular structures and protonation state of 2-Mercaptopyridine in aqueous solution," *Chem. Phys. Lett.*, vol. 647, pp. 103–106, 2016.

[78] N. Bergmann, S. Bonhommeau, K. M. Lange, S. M. Greil, S. Eisebitt, F. de Groot, M. Chergui, E. F. Aziz, "On the enzymatic activity of catalase: an iron L-edge X-ray absorption study of the active centre.," *Phys. Chem. Chem. Phys.*, vol. 12, no. 18, pp. 4827–4832, 2010.

[79] R. Golnak, J. Xiao, M. Pohl, C. Schwanke, A. Neubauer, K. M. Lange, K. Atak, E. F. Aziz, "Influence of the outer ligands on metal-to-ligand charge transfer in solvated manganese porphyrins," *Inorg. Chem.*, vol. 55, no. 1, pp. 22–28, 2016.

[80] K. Atak, R. Golnak, J. Xiao, E. Suljoti, M. Pflüger, T. Brandenburg, B. Winter, E. F. Aziz, "Electronic structure of hemin in solution studied by resonant X-ray emission spectroscopy and electronic structure calculations.," *J. Phys. Chem. B*, vol. 118, no. 33, pp. 9938–9943, 2014.

[81] V. N. Strocov, T. Schmitt, U. Flechsig, T. Schmidt, A. Imhof, Q. Chen, J. Raabe, R. Betemps, D. Zimoch, J. Krempasky, X. Wang, M. Grioni, A. Piazzalunga, L. Patthey, "High-resolution soft X-ray beamline ADRESS at the Swiss Light Source for resonant inelastic X-ray scattering and angle-resolved photoelectron spectroscopies," *J. Synchrotron Radiat.*, vol. 17, no. 5, pp. 631–643, 2010.

[82] S. Schreck, A. Pietzsch, B. Kennedy, W. Quevedo, P. S. Miedema, C. Såthe, S. Techert, J. A. Terschlüsen, V. N. Strocov, T. Schmitt, F. Hennies, J.-E. Rubensson, P. Wernet, A. Föhlisch, "Ground state potential energy surfaces around selected atoms from resonant inelastic X-ray scattering.," *Sci. Rep.*, vol. 6, p. 20054, 2016.

[83] R. Alonso-Mori, D. Sokaras, D. Zhu, T. Kroll, M. Chollet, Y. Feng, J. M. Glownia, J. Kern, H. T. Lemke, D. Nordlund, A. Robert, M. Sikorski, S. Song, T. C. Weng, U. Bergmann, "Photon-in photon-out hard X-ray spectroscopy at the Linac Coherent Light Source," *J. Synchrotron Radiat.*, vol. 22, pp. 612–620, 2015.

[84] T. Schmitt, F. M. F. de Groot, J. E. Rubensson, "Prospects of high-resolution resonant X-ray inelastic scattering studies on solid materials, liquids and gases at diffraction-limited storage rings.," *J. Synchrotron Radiat.*, vol. 21, no. Pt 5, pp. 1065–1076, Sep. 2014.

IntechOpen

IntechOpen